

## ELECTRONIC SUPPLEMENTARY INFORMATION

### **3-D Flowerlike Architectures Constructed by Ultrathin Perpendicularly Aligned Mesoporous Nanoflakes for Enhanced Asymmetric Catalysis**

*Lei Zhang,<sup>a</sup> Yanan Guo,<sup>b</sup> Juan Peng,<sup>a</sup> Xiao Liu,<sup>a</sup> Pei Yuan,<sup>b</sup> Qihua Yang<sup>\*a</sup> and Can Li<sup>\*a</sup>*

<sup>a</sup> State Key Laboratory of Catalysis, Dalian Institute of Chemical Physics, Chinese Academy of Sciences, 457 Zhongshan Road, Dalian 116023, China

<sup>b</sup> Centre for Microscopy and Microanalysis and ARC Centre of Excellence for Functional Nanomaterials, University of Queensland, Brisbane, Queensland 4072, Australia

## Part 1: Synthesis and characterization of 3-D Flowerlike Architectures

**a. Chemicals.** Tetraethoxysilane (TEOS, 99%), cetyltrimethylammonium bromide (CTAB, 95%), calcium oxide (CaO, 99%), sodium hydroxide (98%), and diethylzinc ( $\text{Et}_2\text{Zn}$ , 1 M in hexane) were purchased from Sigma-Aldrich. Benzaldehyde was purchased from Acros Company (USA).  $\text{Ti}(\text{O}i\text{Pr})_4$  was purchased from Alfa-Aesar (USA) and was distilled before use.  $(R)$ - $(+)$ -1,1'-bi-2-naphthol ( $R$ - $(+)$ -Binol) was obtained from Lianyungang Chiral Chemicals Company (China). 3-Chloropropyltrimethoxysilane was obtained from Wuhan Tianmu Science & Technology Development Co. Ltd (China). All the reactions were carried out under an argon atmosphere using standard Schlenk techniques.  $(R)$ - $(+)$ -2,2'-di(methoxymethyl)oxy-6,6'-di(1-propyltrimethoxy silyl)-1,1'-binaphthyl (BSBinol) was synthesized according to the published method.<sup>1</sup>

**b. Synthesis of FMAss-x.** In a typical synthesis, 0.20 g of CTAB was dissolved in 96 g of deionized water under stirring at room temperature. Then 0.1 of CaO (mol ratio of Ca/Si=0.3) was added into the solution, the resulting mixture was ultrasonically irradiated for 10 min under ambient conditions with a ultrasonic cleaning instrument (KUDOS, SK3300H, 59 kHz) immersed directly in the solution (the power used was 160 W). Temperature of the solution was raised to 80 °C. Then, TEOS (1.2g) was added sequentially and rapidly via injection (pH=11.8). After stirring for an additional 2 h, the reaction mixture was transferred into a Teflon-lined autoclave and aged at 110 °C under static conditions for 72 h. The samples were denoted as FMAss-x, where x is the molar ratio of Ca/Si. The surfactant was extracted by refluxing with HCl-ethanol solution at 60 °C for 8 h. The resulting products were collected by filtration and dried at room temperature.

In order to understand the formation mechanism, mesoporous silica nanospheres under similar conditions to FMAss-0.3 was synthesized using NaOH as base. Typically, 0.20 g of CTAB was dissolved in 96 g of deionized water under stirring at room temperature. Then 0.70 mL of NaOH (2 M) was added into the solution (pH=11.7). The following procedure is the same as that for FMAss-x.

**c. Synthesis of *R*-(+)-Binol functionalized organosilica flowers.** Compared with the synthesis of FMAss-x, 1.2 g TEOS silica precursor was replaced by a mixture of TEOS (1.0 g, 4.8 mmol) and BSBinol (0.4 g, 0.57 mmol) in 2.0 g of acetone. The following procedure is the same as that for FMAss-x. The samples were denoted as Binol-FMAss-0.3 and Binol-FMAss-0.9, where 0.3 and 0.9 is the molar ratio of Ca/Si.

**d. Synthesis of *R*-(+)-Binol functionalized mesoporous bulk materials.<sup>2</sup>** A mixture (8.5 mmol of Si) of TEOS (1.42 g, 6.8mmol) and BSBinol (0.596 g, 0.85 mmol) in acetone (2.0 g) was added to an aqueous solution containing CTAB (0.36 g), NaOH (0.08 g) and deionized water (9 g) at 30 °C (pH=13.3). After stirring for 12 h at 30 °C, the reaction mixture was transferred into Teflon-lined autoclave and aged at 110 °C under static conditions for 72 h. The following procedure is the same as that for FMAss-x.

**e. Characterization.** X-ray diffraction (XRD) measurements were performed on a Rigaku RINT D/Max-2500 powder diffraction system using Cu Ka radiation. Scanning electron microscopy (SEM) images of samples coated with platinum were recorded on a FEI Quanta 200F microscope. Transmission electron microscopy (TEM) and high resolution transmission electron microscope (HRTEM) images were obtained by FEI Tecnai G2 Spirit at an acceleration voltage of 120 kV and FEI Tecnai F30 electron microscope. The powder samples for the TEM measurements were suspended in ethanol and then dropped onto copper grids with holey carbon films. Nitrogen sorption isotherms of samples were obtained by a Micromeritics ASAP 2020 system analyzer at -196 °C. The BET surface area was calculated using experimental points at a relative pressure of  $P/P_0=0.05-0.25$ . The total pore volume was calculated by the  $N_2$  amount adsorbed at the highest  $P/P_0$  ( $P/P_0 \approx 0.99$ ). The pore size distribution was calculated by the BJH method. Solid-state  $^{13}C$  (100.5 MHz) cross-polarization magic angle-spinning (CP/MAS) nuclear magnetic resonance (NMR) and solid-state  $^{29}Si$  (79.4 MHz) magic angle-spinning (MAS) NMR experiments were recorded on a Varian infinity-plus 400 spectrometer equipped with a magic-angle spin probe in a 4 mm ZrO<sub>2</sub> rotor. The experimental parameters for  $^{13}C$  CP/MAS NMR experiments were 10-kHz spin rate, 2-s pulse delay, 6-min contact

time and 1000-2000 scans and for  $^{29}\text{Si}$  MAS NMR experiments were 8- kHz spin rate, 4-s pulse delay, 10-min contact time and 3000-5000 scans. Infrared spectra were recorded on a Thermo Nicolet Nexus 470 Fourier transform infrared (FTIR) spectrometer. C, H, and N element analysis was performed on varioEL III.

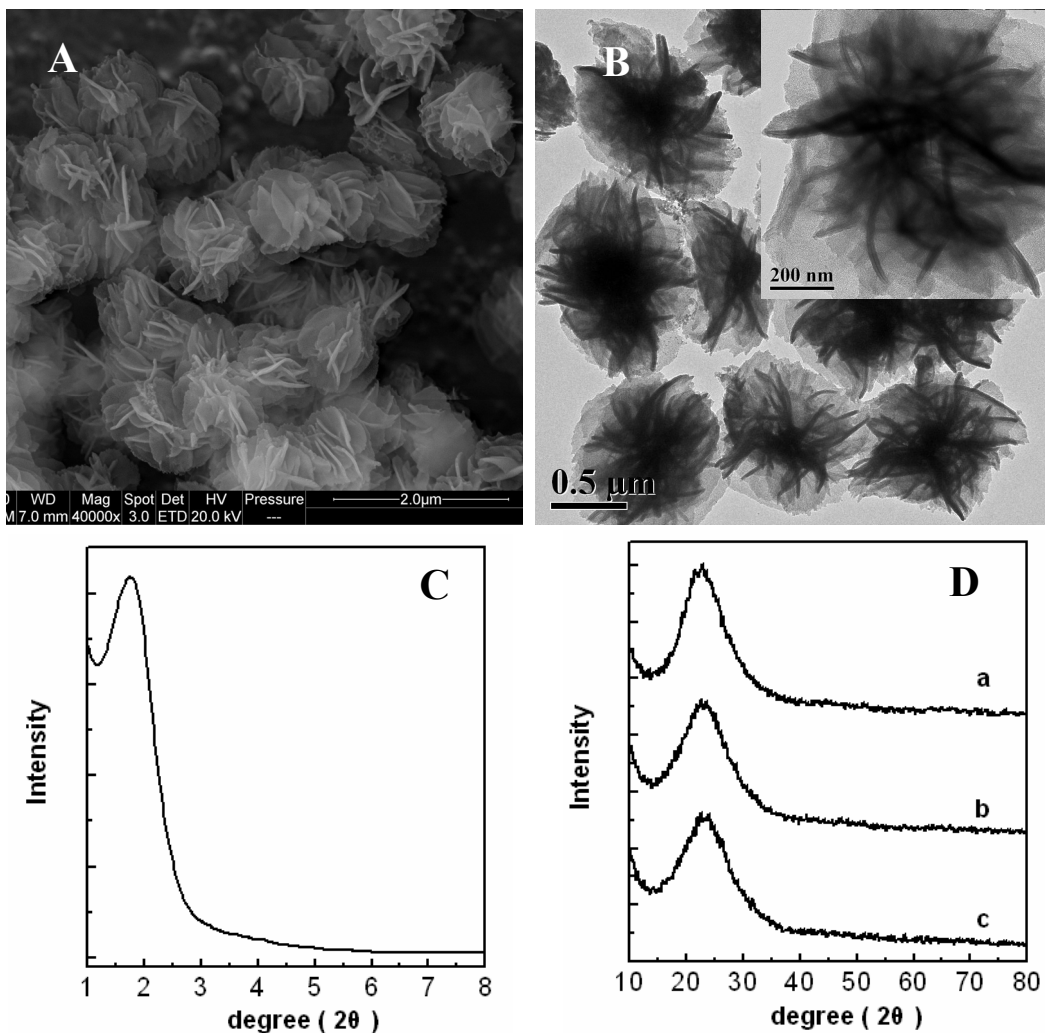


**Fig. S1.** SEM (A), TEM (B) and low angle XRD patterns (C) of extracted FMA-0.3; Wide-angle XRD patterns (D) of extracted FMA-x: FMA-0.15 (a), FMA-0.3 (b) and FMA-0.9 (c).

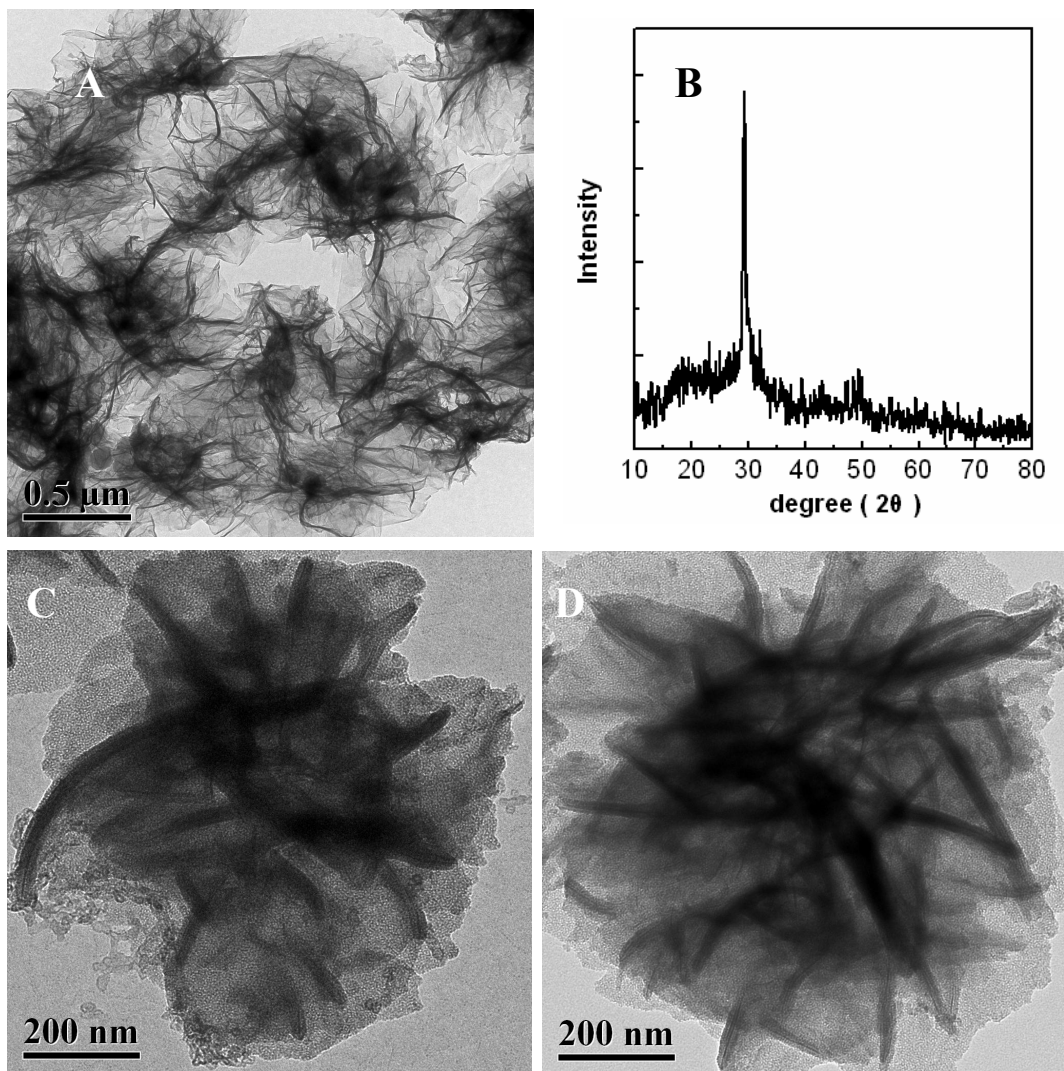


**Fig. S2.** Cryo-TEM images of samples taken out at different reaction time during the synthesis of FMA-0.3: the sample taken out immediately after the addition of TEOS (A), 2 min (C) and 30 min (D); wide angle XRD patterns (B) of immediate precipitation after the addition of TEOS.

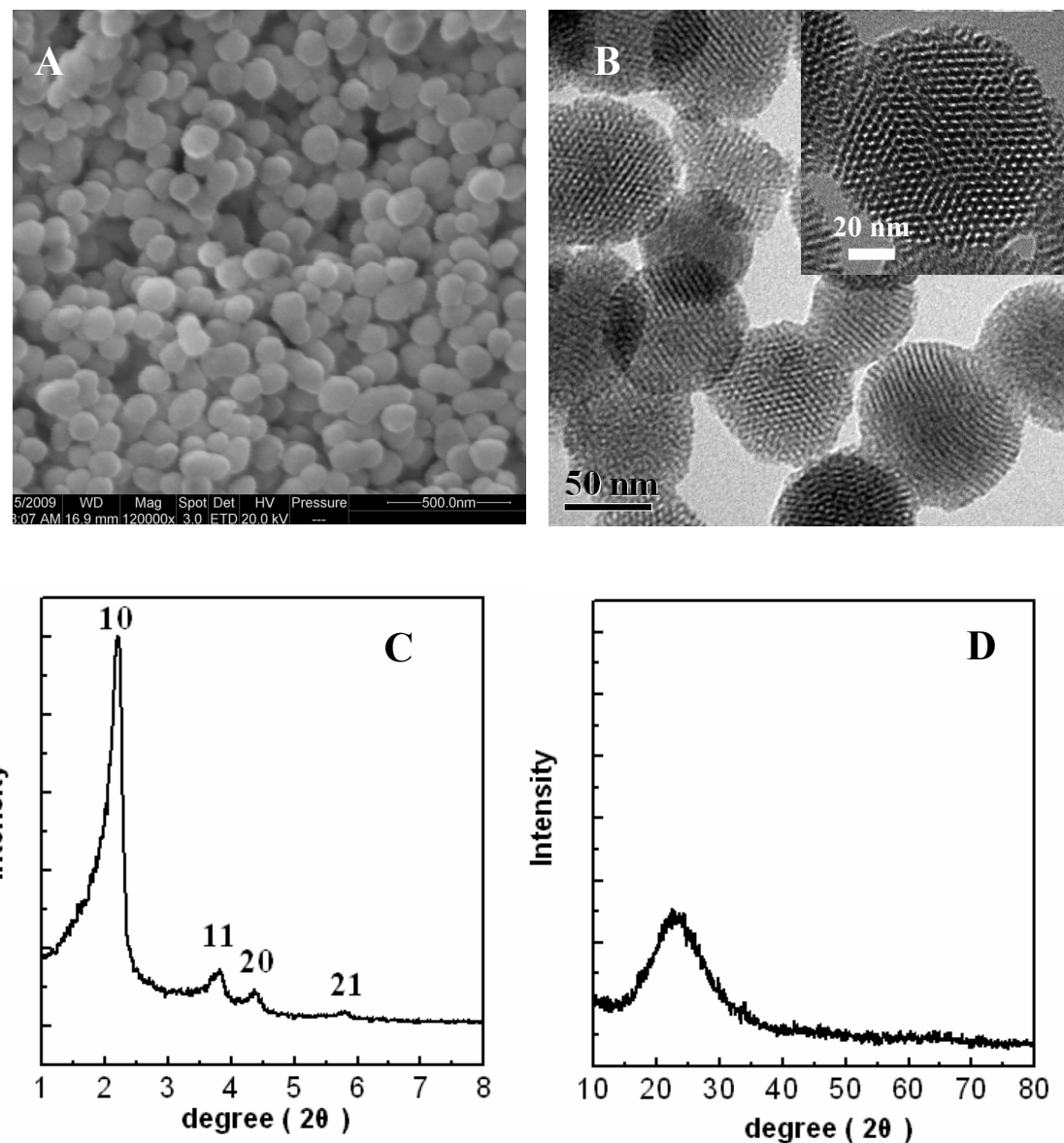


**Fig. S3.** SEM, TEM, low angle XRD patterns and wide angle XRD patterns of as-synthesized mesoporous silica nanospheres synthesized using NaOH as base.

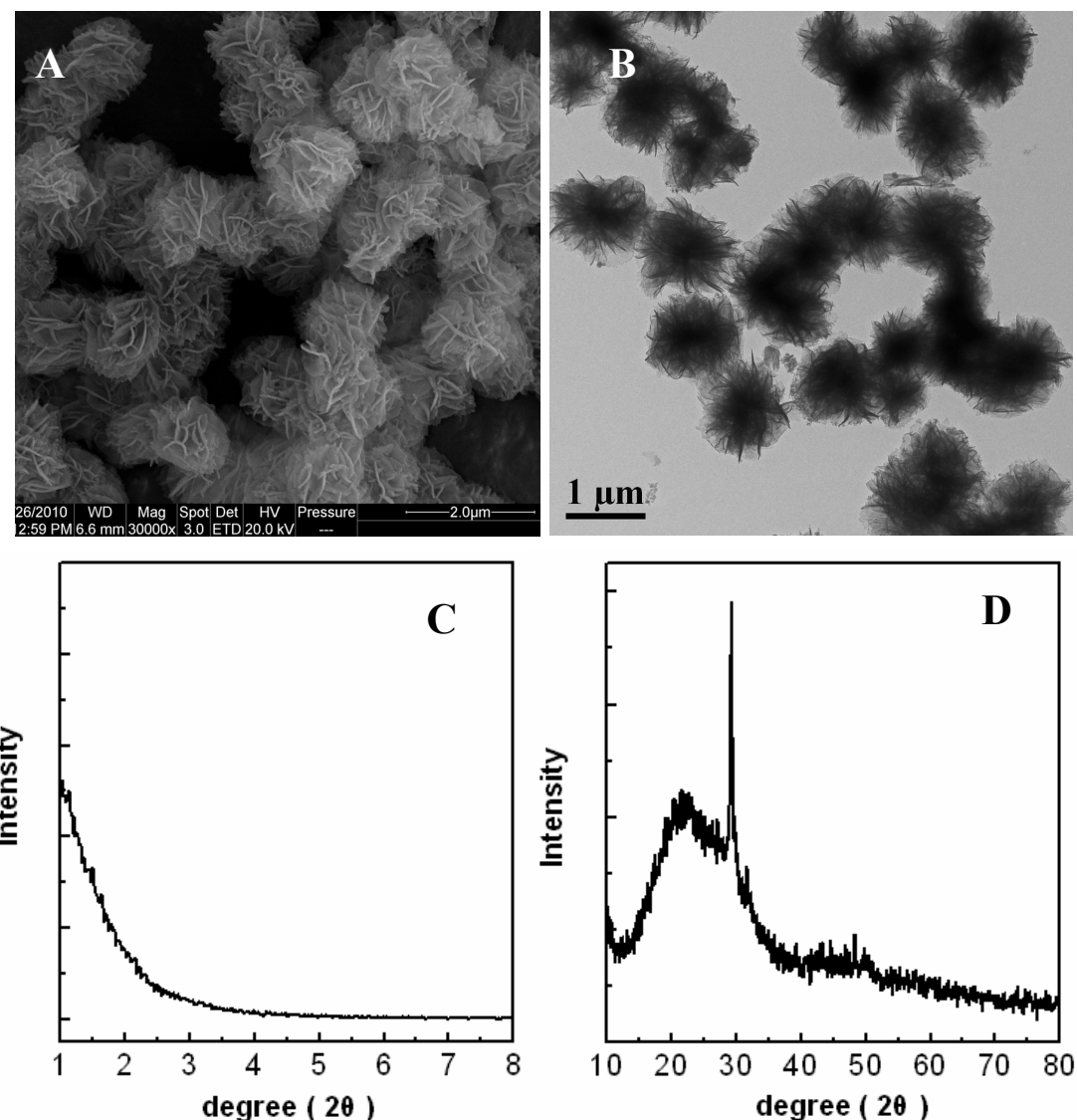


**Fig. S4.** SEM, TEM, low angle XRD patterns and wide angle XRD patterns of as-synthesized 3-D flowerlike nanostructures constructed by nanoflakes under similar conditions to FMAss-0.3 but without using CTAB. No diffraction peaks could be observed in the low angle diffraction region, indicating that this sample have disordered structure. The peak at 25° is assigned to amorphous silica and the peak at 30° are well indexed to  $\text{Ca}_3\text{Si}_2\text{O}_7\text{-xH}_2\text{O}$  (JCPDS 33-0306).<sup>3</sup>

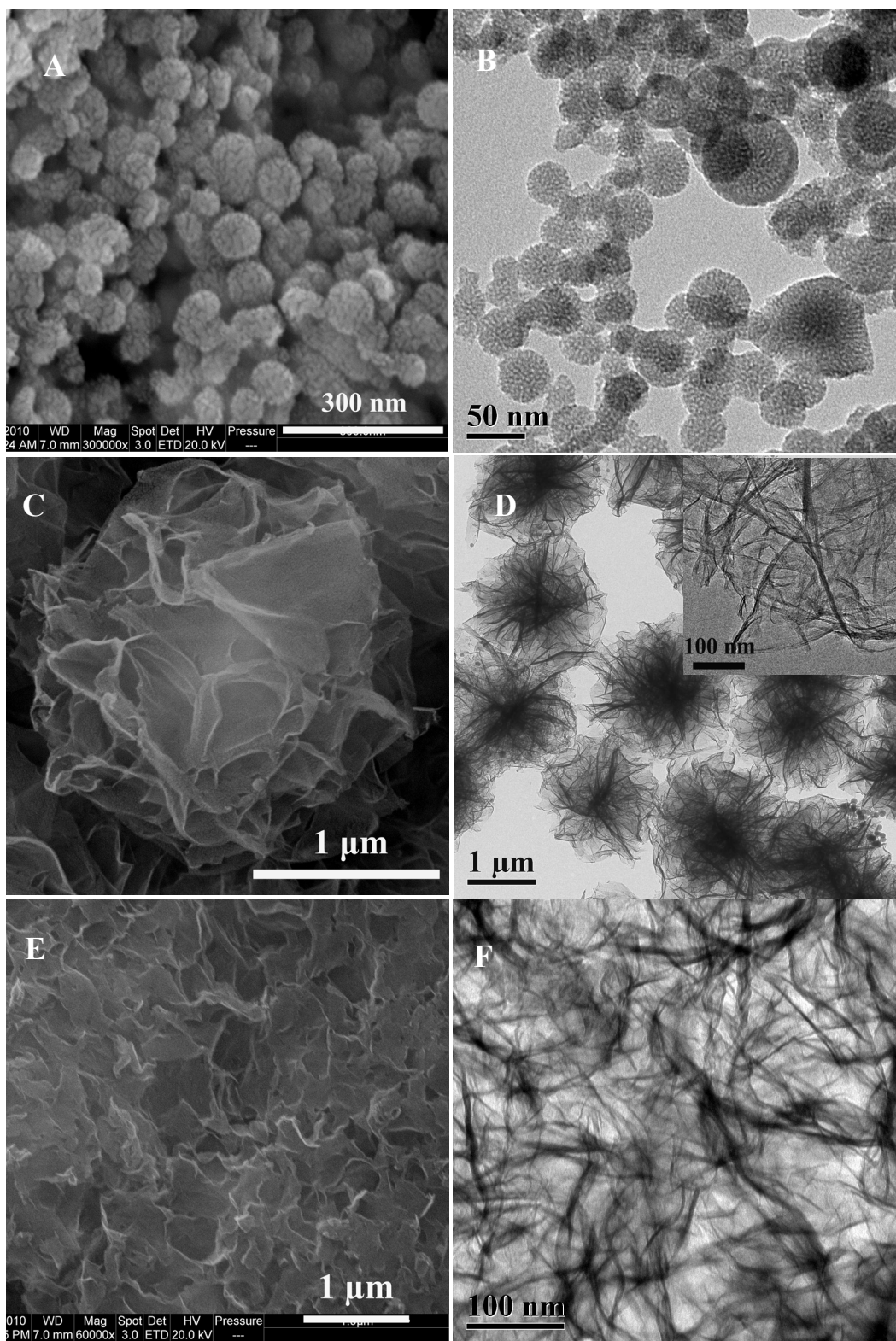


**Fig. S5.** SEM images (A, C and E) and TEM images (B, D and F) of as-synthesized FMA samples: FMA-0.15 (A, B), FMA-0.9 (C, D), and FMA-1.5 (E, F).

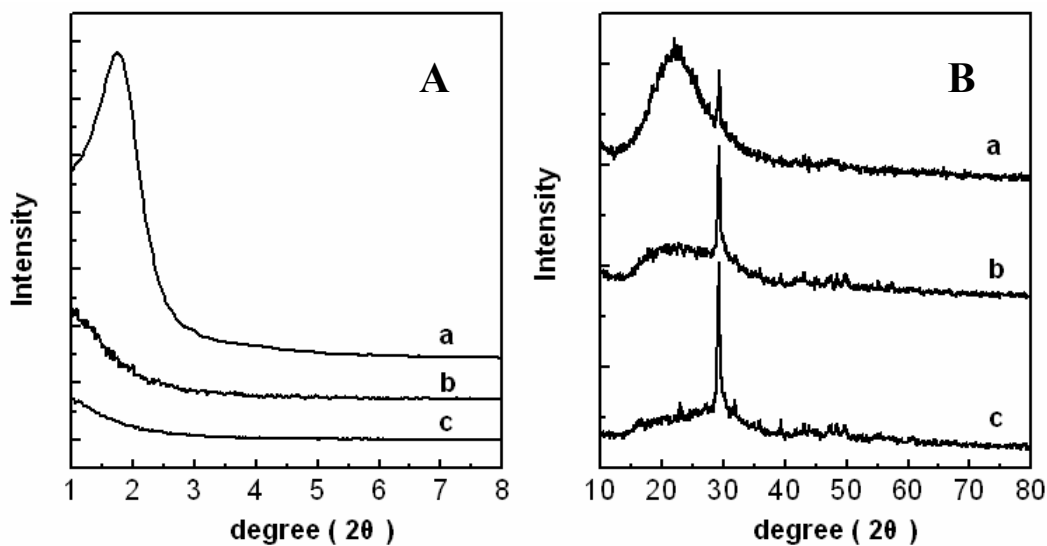


**Fig. 6.** Low angle XRD patterns and wide-angle XRD patterns of as-synthesized FMAss-x: FMAss-0.15 (a), FMAss-0.9 (b) and FMAss-1.5(c).

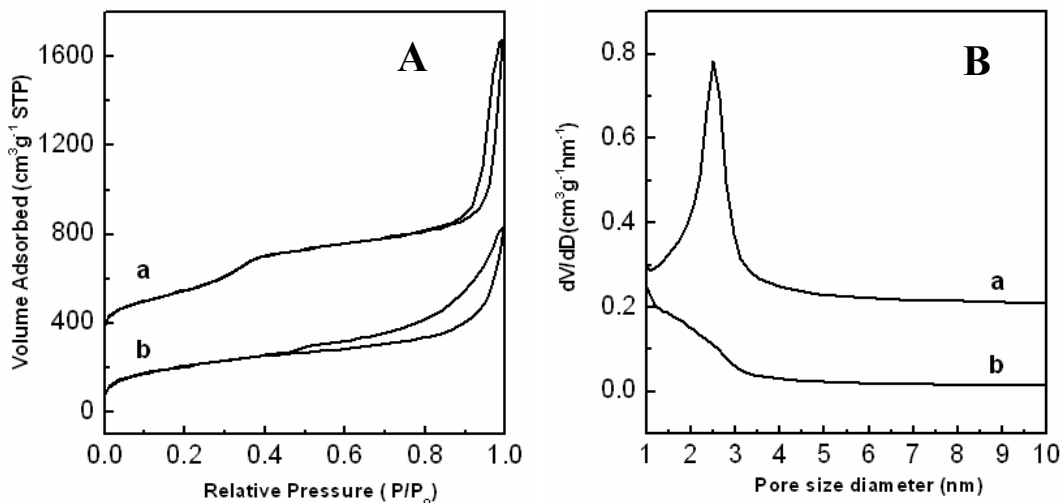


**Fig. S7.** N<sub>2</sub> adsorption/desorption isotherms (A), and pore size distribution from adsorption branch (B) of surfactant-extracted FMAss-x: FMAss-0.15 (a) and FMAss-0.9 (b). Isotherms of (a) in (A) have been offset  $300 \text{ cm}^3 \text{g}^{-1}$  along the vertical axis for clarity.

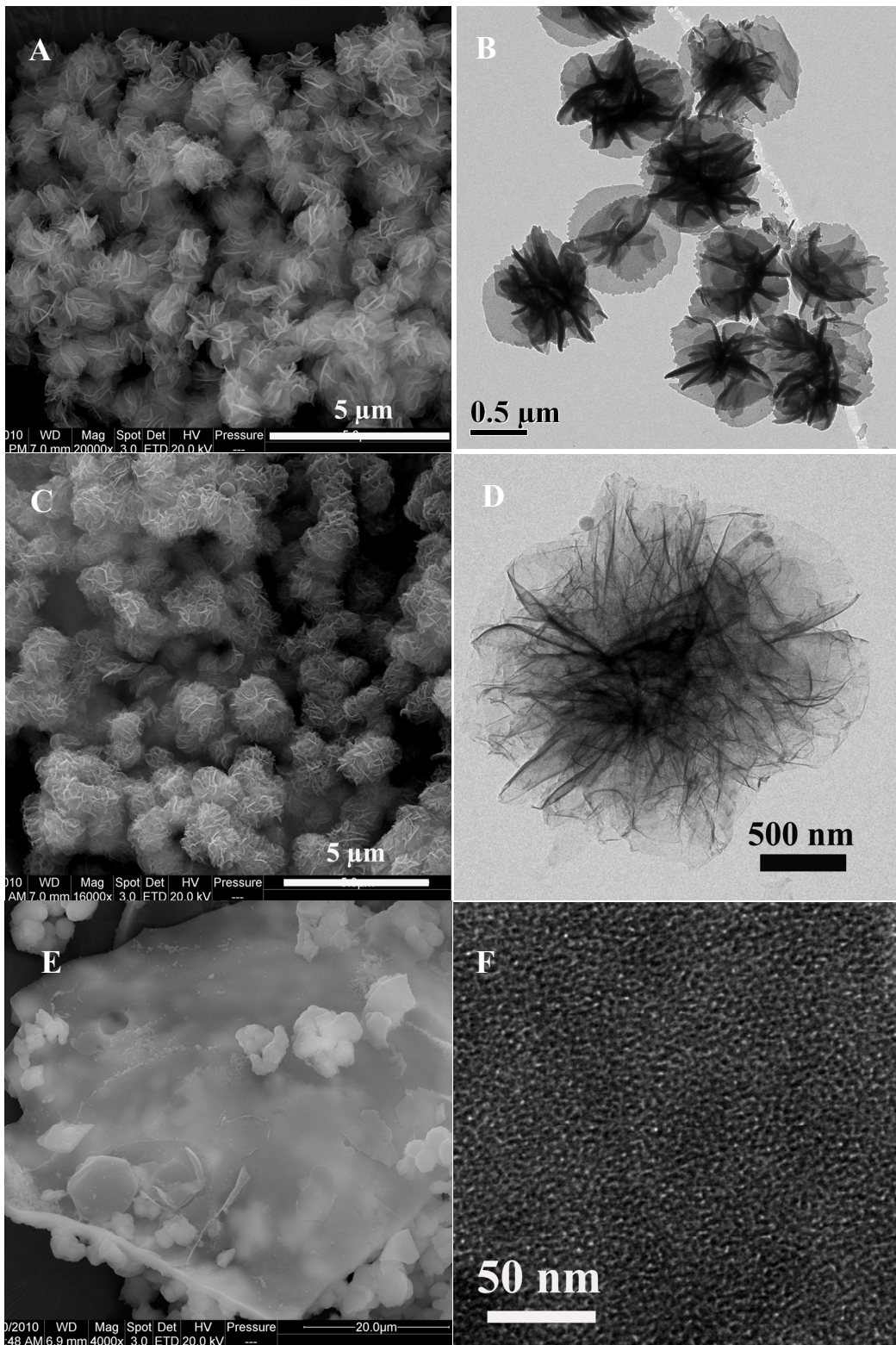


**Fig. S8.** SEM images (A, C and E) and TEM images (inset of B, D and F) of surfactant-extracted *R*-(+)-Binol functionalized organosilicas: Binol-FMAs-0.3 (A, B), Binol-FMAs-0.9 (C, D) and mesoporous bulk materials (E, F).

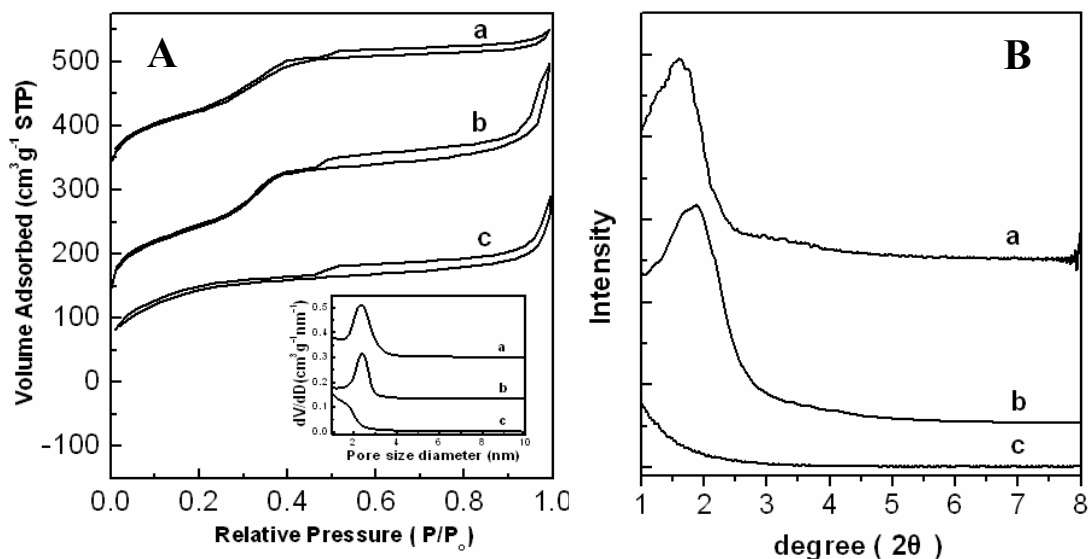


**Fig. S9.** N<sub>2</sub> adsorption/desorption isotherms (A), pore size distribution from adsorption branch (inset of A) and Low angle XRD patterns (B) of surfactant-extracted *R*-(+)-Binol functionalized organosilicas: mesoporous bulk materials (a), Binol-FMAs-0.3 (b) and Binol-FMAs-0.9 (c). Isotherms of (a) and (b) in A have been offset by 250 and 50 cm<sup>3</sup>g<sup>-1</sup> along the vertical axis for clarity, respectively.

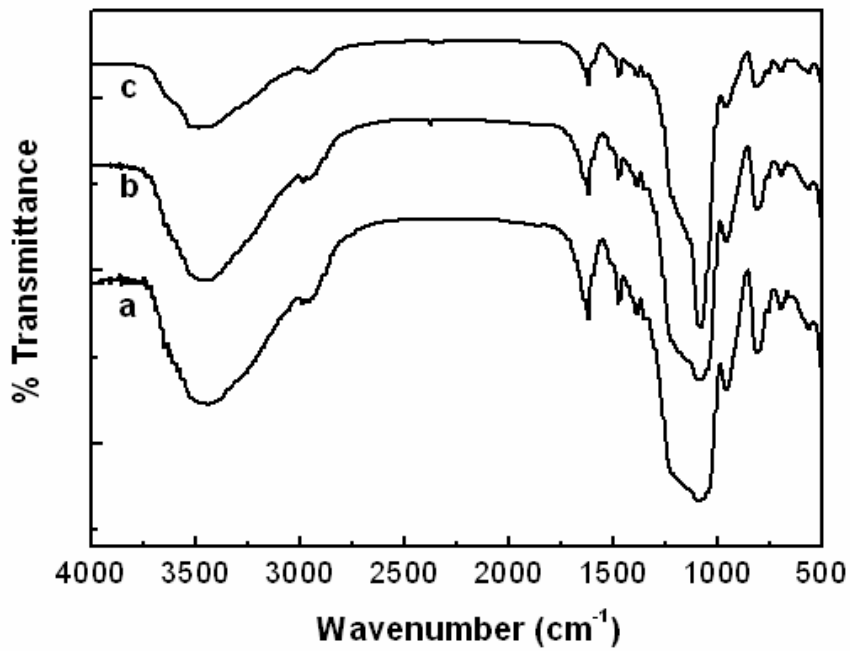


**Fig. S10.** FT-IR spectra of surfactant-extracted *R*-(+)-Binol functionalized organosilica flowers: Binol-FMAs-0.3 (a), Binol-FMAs-0.9 (b) and mesoporous bulk materials (c).

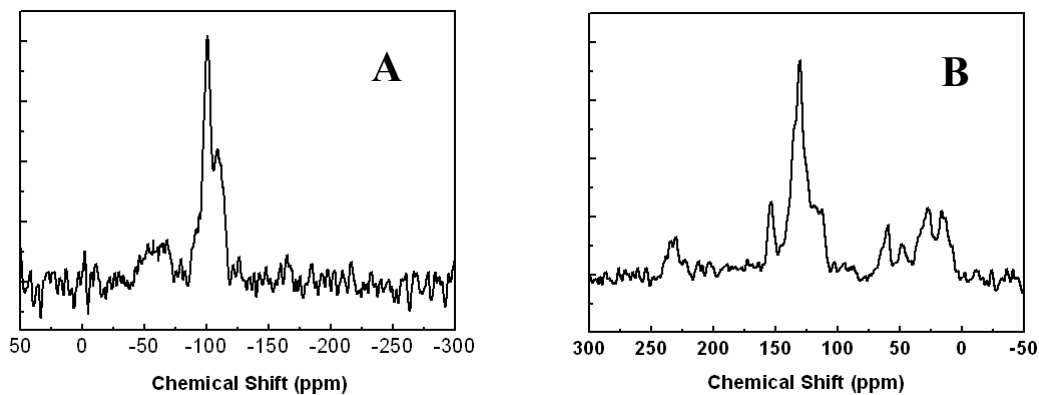


**Fig. S11.**  $^{29}\text{Si}$  MAS NMR (A) and  $^{13}\text{C}$  CP/MAS NMR spectra (B) of surfactant-extracted Binol-FMAs-0.3.

**Table 1.** Physicochemical parameters of surfactant-extracted samples.

Samples	Particle Size (nm)	d spacing value (Å)	Surface Area ( $\text{m}^2\text{g}^{-1}$ )	Pore Size (nm)	Pore Volume ( $\text{cm}^3\text{g}^{-1}$ )
FMAs-0.15	20~30	5.0	867	2.6	2.1
FMAs-0.3	1000	4.9	813	2.6	1.3
FMAs-0.9	1000	-	737	-	1.3
FMAs-1.5	>10000	-	-	-	-
Binol-FMAs-0.3	1000	4.7	531	2.5	0.6
Binol-FMAs-0.9	1000	-	526	-	0.4
Bulk materials	>10000	5.5	460	2.5	0.4

**Part 2: Ti-promoted asymmetric addition of diethylzinc to benzaldehyde on R-(+)-Binol functionalized organosilicas.** The catalytic properties of Binol-FMAs-0.3, Binol-FMAs-0.9 and mesoporous bulk materials were investigated in Ti-promoted asymmetric addition of diethylzinc to aldehydes. After drying under vacuum at 120 °C for 3 h, the solid catalyst was stirred in 4 ml of CH<sub>2</sub>Cl<sub>2</sub> containing Ti(O*i*Pr)<sub>4</sub> (1.5 mmol) at room temperature for 2 h under an argon atmosphere. After addition of Et<sub>2</sub>Zn (1 M solution in hexane, 3.0 mmol), the mixture was cooled to 0 °C, followed by dropwise addition of aldehyde (1.0 mmol). The reaction mixture was stirred at 0 °C. The aliquot (0.5 mL) was taken out by syringe at desired time and was mixed with saturated NH<sub>4</sub>Cl solution (1.0 ml) to stop the reaction. The solid was filtered off and washed with CH<sub>2</sub>Cl<sub>2</sub>. The organic layer was separated from the filtrate and dried over anhydrous Na<sub>2</sub>SO<sub>4</sub>. The yield and enantiomeric excess of the product were measured on an Agilent 6890 gas chromatograph equipped with a flame ionization detector and an HP-Chiral 19091GB213 capillary column.

**Table 2.** Ti-promoted asymmetric addition of diethylzinc to benzaldehyde on surfactant-extracted Binol-FMAs-0.3, Binol-FMAs-0.9 and mesoporous bulk materials.<sup>[a]</sup>

Samples	Time (h)	Binol content <sup>[b]</sup> (mmol g <sup>-1</sup> )	Conversion <sup>[c]</sup> (%)	Ee <sup>[c]</sup> (%)	TOF <sup>[d]</sup> (h <sup>-1</sup> )
Binol-FMAs-0.3	4	0.74	99	87	23
Binol-FMAs-0.9	6	0.75	86	70	5
Bulk materials	6	0.36	36	33	1

[a] all the reactions were carried out in CH<sub>2</sub>Cl<sub>2</sub> with Ti(O*i*Pr)<sub>4</sub> (1.5 mmol), Et<sub>2</sub>Zn (3.0 mmol) and benzaldehyde (1.0 mmol) at 0 °C. The molar ratio of Ti to ligand is 13. [b] Determined by elemental analysis based on the C contents. [c] Conversions and ee values were determined by GC on a HP-Chiral 19091G-B213 capillary column. [d] TOF was calculated according to the following equation: TOF = Mmol of conversed benzaldehyde/(Mmol of Binol\*h).

## Reference

- [1] (a) H. Ishitani, M. Ueno and S. Kobayashi, *J. Am. Chem. Soc.*, 2000, **122**, 8180; (b) X. Liu, P. Y. Wang, Y. Yang; P. Wang and Q.H. Yang, *Chem. Asian J.*, 2010, **5**, 1234.
- [2] J. Liu, J. Yang, Q.H. Yang, G. Wang and Y. Li, *Adv. Funct. Mater.*, 2005, **15**, 1297.
- [3] J. Wu, Y. J. Zhu, S.W. Cao and F. Chen, *Adv. Mater.*, 2010, **22**, 749-753.